



HAL
open science

Transport properties in molten carbonates: self-diffusion and conductivity measurements at high temperature

A. Zhadan, V. Sarou-Kanian, L. del Campo, L. Cosson, M. Malki, C. Bessada

► To cite this version:

A. Zhadan, V. Sarou-Kanian, L. del Campo, L. Cosson, M. Malki, et al.. Transport properties in molten carbonates: self-diffusion and conductivity measurements at high temperature. *International Journal of Hydrogen Energy*, 2020, 10.1016/j.ijhydene.2020.06.294 . hal-03014103

HAL Id: hal-03014103

<https://hal.science/hal-03014103>

Submitted on 26 Nov 2020

HAL is a multi-disciplinary open access archive for the deposit and dissemination of scientific research documents, whether they are published or not. The documents may come from teaching and research institutions in France or abroad, or from public or private research centers.

L'archive ouverte pluridisciplinaire **HAL**, est destinée au dépôt et à la diffusion de documents scientifiques de niveau recherche, publiés ou non, émanant des établissements d'enseignement et de recherche français ou étrangers, des laboratoires publics ou privés.

Transport properties in molten carbonates: self-diffusion and conductivity measurements at high temperature

A. Zhadan^{1*}, V. Sarou-Kanian¹, L. Del Campo¹, L. Cosson¹, M. Malki¹ and C. Bessada¹

¹Conditions Extrêmes et Matériaux: Haute Température et Irradiation, CEMHTI, UPR 3079 - CNRS Univ Orleans 45071 Orléans, France.

Corresponding author Antonii Zhadan, e-mail: antonii.zhadan@cnrs-orleans.fr

Abstract:

A better understanding and use of molten carbonate fuel cells (MCFCs) requires more detailed consideration on transport properties in melt. The combination of different methodological developments can be one solution to improve our comprehension. Here we present ²³Na and ⁷Li self-diffusion coefficients measured by pulsed field gradient (PFG) NMR technique combined with electrical conductivity obtained by a 4-electrod set up, in the eutectic mixture Li₂CO₃-Na₂CO₃ (52:48 % mol) at high temperature (up to 1050 K), and under pure CO₂ atmosphere. The results were compared with known experimental data from literature obtained by radiotracers techniques and 2-electrod set up and also with some calculations of the transport properties.

Keywords:

Molten carbonates; high temperature; PFG NMR; electrical conductivity; CO₂; self-diffusion

1. Introduction

The capture of CO₂ and its exploitation has become a significant worldwide issue due to environmental reasons, and could supply an inexhaustible energy source [1]. Among the different methods proposed to take advantage of this CO₂ storage, the electrolysis of CO₂ in molten carbonate batteries, the molten carbonate fuel cells (MCFCs) [2], is one of the most efficient solution. Actually, molten carbonates are known to be a good CO₂ solvent. These systems are liquids in very large temperature and pressure ranges. They have low viscosity and a significant capability to dissolve volatile compounds such as water and CO₂ [3,4]. Molten carbonates are difficult to study experimentally because of their high melting temperatures:

from 670 K for the eutectic composition $\text{Li}_2\text{CO}_3\text{-Na}_2\text{CO}_3\text{-K}_2\text{CO}_3$ (43.5-31.5-25 %mol) to 1164 K for pure K_2CO_3 . In addition, these molten salts are corrosive toward different materials usually used for sample holder in different experimental techniques. Cell materials have to fulfil at least three conditions: resisting to high temperature, resisting to the corrosion by the salts and not perturbing the detected signal. The quite recent commercialization of high-quality ceramic materials able to resist to high temperature and to corrosion by molten carbonates has opened new perspectives for spectroscopic and conductivity measurements.

Two experimental techniques were used in this paper for a better understanding of the structure and the dynamics of molten carbonates: nuclear magnetic resonance (NMR) [5] and electrical conductivity measurements both in the liquid state at high temperature [6] up to 1300 K.

Pulsed field gradient NMR at high temperature (HT PFG NMR) particularly provide a valuable insight into the dynamics of molten salt through the measurements of self-diffusion coefficients [7]. This technique is selective and give unique information for each observable nucleus, depending on the mobility of anions and cations in molten carbonates.

The self-diffusion coefficient D , is related to the ability of atoms or groups of atoms to move in their environment. The measurement of D is generally made by the capillary method and radioactive tracers [8]. A radioactive salt is put in a platinum capillary and plunged in the same non-radioactive molten salt. After a selected time of diffusion, the capillary is cooled and solidified, and then is cut in different segments where the radioactivity is counted. This method is precise but difficult to handle. It requires the use of radioactive species whose period may be short. Because of its difficult implementation and the requirement of radioactive tracers, this technique have been limited and the self-diffusion coefficients are now commonly estimated through electrochemical experiments. The development of pulse field gradients (PFG) NMR at high temperature provides different advantages: the selectivity toward the isotope, the direct determination of D over a wide diffusion time range ($10^{-9}\text{-}10^{-10}$ m²/s), and the possibility to perform in situ experiments up to 1000 K.

The results will be connected with electrical conductivity measurements realized by the 4-electrode cell system more adapted for highly conductive liquids at high temperature.

2. Experimental

2.1 Samples preparation

Carbonate mixtures in the binary system $\text{Li}_2\text{CO}_3\text{-Na}_2\text{CO}_3$ were prepared from dried powders Li_2CO_3 (99.998%), Na_2CO_3 (99.997%) from Alfa Aesar. Sodium carbonate is hygroscopic, and all mixtures were prepared in a glove box under dried argon.

For NMR experiments, alumina (Al_2O_3) crucibles were directly filled by carbonates and stored in a gloves box at ambient temperature. For electrical conductivity measurements, the same mixtures of carbonates were melted in alumina crucible under air, and after cooling, stored in the electric oven at 423 K.

2.2 Materials characterization

2.2.1 NMR

High-temperature NMR experiments were performed with a laser heating system developed at CEMHTI, Orleans (France) [9]. This system consists in a Bruker AVANCE I NMR spectrometer (magnetic field of 9.4 T), associated with two CO_2 lasers ($\lambda = 10.6 \mu\text{m}$, 250 W), which allows heating the sample container (crucible) from top and bottom sides, insuring a good homogeneity of temperature inside the crucible.

For other molten salts systems such as fluorides or chlorides, the crucible is made usually from boron nitride (BN) [10] with no interaction and a good thermal conductivity during the experiments. However, in the case of molten carbonates, the salt reacts with BN at high temperature and create dangerous gases such as cyanamides [11]. We have to find new materials for the container, fulfilling the three criteria for high temperature NMR experiments: non-metallic so not shielding the NMR radio frequency; inert toward molten carbonates; good absorption of CO_2 laser for efficient heating; good thermal conductivity insuring temperature homogeneity. Three refractory materials were tested: alumina, zirconia and magnesium oxide.

Alumina has a moderate thermal conductivity and high melting temperature, but it can interact with molten carbonates at temperature higher than 1073 K to create meta-aluminate (MAIO_2) [12]. Zirconia (ZrO_2) is inert to molten carbonates but has a low thermal conductivity. Finally, magnesium oxide (MgO), has a good thermal conductivity and high melting temperature and don't interact with molten carbonates. The geometrical complexity of the crucible with plug, creates some difficulties in the fabrication, but now we find some compromise between the geometry and the quality of MgO , to design specific containers adapted to this experiments. Taking advantages of the properties of Al_2O_3 and MgO , the

crucible is a new configuration associating a closed oxide magnesium crucible with an alumina crucible inside that can be filled in a gloves box under dried argon (Figure 1).

Figure 1.

The NMR spectra were collected for the $\text{Li}_2\text{CO}_3\text{-Na}_2\text{CO}_3$ (52:48 %mol) eutectic composition. The chemical shifts of ^{23}Na and ^7Li were referenced to 1M aqueous solutions of NaCl and LiCl respectively. Samples were heated up to 993 K. For every experiment, the acquisition started after 6 min of heating to be sure that the thermal equilibrium inside the crucible was reached.

Self-diffusion coefficients measurements were performed using PFG NMR technique specifically adapted for molten salts up to high temperature [7, 13]. A Bruker *Diff30* probe specially modified for high temperature experiments was used allowing sufficiently high gradient strengths (up to 1000 G/cm for this study) in conjunction with a convection-free NMR pulse sequence proposed by Jerschow et al. [14] in order to get a proper diffusion measurement.

The self-diffusion coefficient of both cations, ^7Li , and ^{23}Na are registered over at least 300 K above the melting point, by simply changing the resonance frequency. It is just to remark that this technique is more efficient and rapid than the radiotracers diffusion, and don't need to involve any additional treatment of the data, nor destruction of the sample.

For the ^{13}C and ^{17}O self-diffusion measurement, the challenge will be the enrichment of the sample by these two isotopes. ^{17}O , the only observable isotope of oxygen, with 0.037% of natural abundance, will not allow any direct measurement, while for the ^{13}C isotope of carbon, 1.11% abundant, some commercial Na_2CO_3 and Li_2CO_3 enriched by ^{13}C , are now available, and it will be the aim of another paper. For this study, at first we will use the experimental data obtained by Spedding et al. [15] for CO_3^{2-} by capillary method.

From our measurements we will extract the diffusion coefficients for both alkali, and the corresponding activation energies. They will be compared with experimental and theoretical data from literature.

2.2.2 Electrical conductivity

Impedance spectra were recorded using a SOLARTRON SI 1260 spectrometer in the frequency range of 1Hz to 1MHz. The conductivity cell used for our measurements, constituted of 4 Pt-electrodes, is described in [16]. This set up is specifically adapted for measurements of the electrical conductivity of highly conductive liquids at high temperatures. The outermost

electrodes are two plates imposing a current flow whereas the innermost electrodes are two wires measuring the voltage drop. The use of a four electrode set up minimizes the polarization effects at the sample/electrode interface. In theory, such polarization effects should disappear with 4 electrodes but classical plots of the real vs. the imaginary part of the complex impedance do show small residual polarization effects for frequencies below ~10 Hz.

Sample temperatures were measured by a platinum thermocouple (type S) covered by an alumina sheath that was inserted into the system of crucibles containing the melt. This system consists of two alumina crucibles and one steel crucible. The first alumina crucible contains the carbonate sample, the second metallic one protects the guard crucible from the molten salts which could get in, if the first alumina crucible breaks. The third (and last) alumina guard crucible protects the oven from both, the molten carbonates and the gases. All measurements were made under 1 atm CO₂ in the temperature range from about 373 K to about 1023 K. The conductivity cell was calibrated by the 1M KCl solution at room temperature for different depth of immersion of electrodes. Details of the measurement procedure have been reported in the literature [17, 18].

3. Results and discussion

3.1 ²³Na and ⁷Li NMR spectra

²³Na and ⁷Li spectra at different temperatures are presented in Figure 2. At room temperature the NMR lines are very broad for both nuclei. It is explained by the presence of dipolar and quadrupolar NMR interactions in the solid state carbonate mixture. Before the melting temperature, the line becomes narrow due to the increase of the cations mobility, and the progressive averaging of the dipolar and quadrupolar couplings. When the salt is completely melted, the NMR interactions except the chemical shift one are averaged to zero, yielding to a single sharp line. At high temperature the different ionic species present in the system are in rapid exchange (few picoseconds), compared to the time scale of the NMR measurements (10⁻⁹ s). As a result, the NMR line corresponds to the average of all possible ionic configurations experienced by the observed nucleus.

Figure 2.

The evolution of ⁷Li and ²³Na chemical shifts with temperature are presented in Figure 3. The chemical shifts decrease slightly with temperature in a very narrow range (~ 1 ppm) such

that it is difficult to state if the present variation of chemical shift with temperature results from physical (density) or chemical (local structure composition) changes.

Figure 3.

3.2 ^{23}Na and ^7Li PFG NMR

As far as we know, this is the first time that the self-diffusion coefficient for both Li^+ and Na^+ ions in molten alkali carbonate $\text{Li}_2\text{CO}_3\text{-Na}_2\text{CO}_3$ (52:48 %mol) eutectic mixture has been reported in the literature. Experimental diffusivity data provided by Spedding et al. [15], who measured the self-diffusion coefficients of Na^+ and CO_3^{2-} ions in molten binary alkali carbonate $\text{Li}_2\text{CO}_3\text{-Na}_2\text{CO}_3$ (52:48 %mol) by capillary diffusion apparatus [8], and diffusivity data calculated by molecular dynamics simulations (Desmaele et al. [19]) were compared with the results of the present work in Figure 4.

Figure 4.

The values of D_{Na} and D_{Li} are in the same order of magnitude than other alkali salts ($10^{-9}\text{m}^2/\text{s}$) [7, 13]. For both cations, D increases with temperature increase, confirming the thermal activation. It is worth noting that in our case, sodium cations diffuse more rapidly than lithium ones, which contradicts the simulation results [19]. Given the smaller size of lithium, it would be expected that it diffuses more quickly than sodium. Nevertheless, lithium has a higher ionic potential than sodium [20], such that the lifetimes of the Li solvation shell is longer than that of Na.

The Arrhenius plot (figure 5) of D vs T provides an activation energy of 0.22 ± 0.01 eV and 0.23 ± 0.02 eV for sodium and lithium, respectively. The activation energy for D_{Na} given by Spedding et al. [15] is higher, of about 0.48 eV, and Desmaele et al. [19] reported values between 0.33 and 0.4 eV for the Na^+ and Li^+ cations. Spedding et al. published also some experimental values for the carbon diffusion, attributed to the CO_3^{2-} anion. The values reported for Na^+ and CO_3^{2-} are of the same order, and suggests some kind of joint action between cations and anions. The diffuse motion in this melt occurs as a result of some combined action that can be related to the vacancy mechanism, cluster movement or ion-pair motion. In the very next future, we will measure the ^{13}C self-diffusion coefficients for CO_3^{2-} , in order to validate this assumption.

Figure 5.

3.3 Electrical conductivity measurements

Conductivity measurements of molten $\text{Li}_2\text{CO}_3\text{-Na}_2\text{CO}_3$ (52:48 %mol) eutectic mixture were performed in the temperature range from 750 to 1050 K. The lower limit in temperature is imposed by the solidification of the sample. Impedance measurements were performed for frequencies ranging from 1 Hz to 1 MHz. The method of determination of static conductivity consists in representing the impedance in the complex plane. In the case of an ideal solid electrolyte, the electrical properties can be simulated by a simple parallel RC circuit, and the presentation of the impedance in the complex diagram (Cole-Cole representation) is an arc whose intersection with the real axis gives access to the dc-resistance of the sample. In our case, the plot of the imaginary part of the impedance as a function of its real part corresponds to an arc of a circle, but whose centre is slightly below the real axis, indicating a deviation from Debye behaviour [21]. At high temperature, the impedance of the sample is too small and the spectra exhibit a vertical line caused by the electrode inductance at high frequencies [22].

This representation also makes it possible to check the absence of contribution of the sample-electrode interface in the studied frequency range. A typical example of the obtained graph is shown in Figure 6 for $\text{Li}_2\text{CO}_3\text{-Na}_2\text{CO}_3$ (52:48 %mol) eutectic mixture at different temperatures. In the absence of new contributions at lower frequencies, the intersection of the arc with the real axis gives a good approximation of the static resistance at the given temperature, and therefore provides the conductivity of the carbonate mixture by the multiplication with the geometric factor of the sample.

Figure 6.

The values of the static conductivity as a function of temperature are presented on figure 7 and are compared with previous results obtained by Kojima et al. [23]. These authors used the 2-electrode method requiring corrections on the measured resistance. Our data are slightly higher than those of Kojima et al., which is not unexpected as the 4-electrode method used in this work avoids the wire resistance contribution to the impedance of the sample contrary to the system used by Kojima et al. [23]. Our measurements are thus believed to be more accurate, even the difference is rather small (about 5% at 1000 K).

Figure 7.

The conductivity values were fit to Arrhenius equation:

$$\sigma = \sigma_0 \exp\left(-\frac{E_a}{kT}\right) \quad (1)$$

where σ (S.cm⁻¹) is the conductivity of the molten carbonate, σ_0 (S.cm⁻¹) a pre-exponential factor, E_a (eV) is the activation energy, k (J.K⁻¹) the Boltzmann constant and T (K) is the absolute temperature. Table 1 shows the obtained results of pre-exponential factor and activation energy. It can be noticed that the activation energy of the electrical conductivity is in close agreement with activation energies extracted from self-diffusion coefficients of Li⁺ and Na⁺, suggesting that the conductivity is mainly controlled by the mobility of these cations. On the other hand, E_a and σ_0 of this study are in very good agreement with the corresponding values reported by Kojima et al. [23].

Table 1.

3.4 Discussion

The electrical conductivity of molten carbonates is related to other transport properties such as self-diffusion. So as to compare these properties, the density measurements on molten Li₂CO₃-Na₂CO₃ (52:48 %mol) eutectic point at 1 atm performed by Kojima et al. [23] are used. The “ideal” electrical conductivity σ^{NE} being related to the self-diffusion coefficients by the Nernst-Einstein equation:

$$\sigma^{NE} = \frac{q^2}{k_B T V} \sum_s N_s z_s^2 D_s \quad (2)$$

where q is the elementary charge, N_s is the number of ions contained in the volume V , z_s is the conduction charge and D_s are the experimental self-diffusion coefficients for the chemical species, and $s = \text{Li}^+, \text{Na}^+ \text{ and } \text{CO}_3^{2-}$ respectively. In order to compare experimentally obtained conductivities to those obtained by the Nerst-Einstein equation, we have used our NMR self-diffusion measurements for sodium and lithium show in figure 4 and data given by Spedding et al. [15] for CO₃²⁻(table 2). The results of the “ideal” electrical conductivity compared to the experimentally obtained values for three different temperatures are presented in table 2.

Table 2.

The Haven ratio contains information about the correlation and the whole atomic mechanism of ionic motion. For the Li₂CO₃-Na₂CO₃ (52:48 %mol) eutectic mixture the value of the Haven ratio is around 0.7 which is very close to the value obtained by Desmaele et al. [19] by ab-Initio calculation. A value of H less than 1 is generally explained by a large contribution of the anticorrelations between ions of the same charge. Moreover, Table 2 shows

that H is practically invariant with temperature suggesting that the transport mechanism of cations and anions does not change with temperature.

4. Conclusions

In this paper we reported, Na^+ and Li^+ self-diffusion coefficients measurements in molten $\text{Li}_2\text{CO}_3\text{-Na}_2\text{CO}_3$ (52:48 %mol) eutectic mixture were combined with electrical conductivity using 4-electrode experimental set up at temperatures ranging from 770 to 1000 K

Increasing temperature influence values of the conductivity and self-diffusion coefficients. In the first approximation, the value of Haven ratio calculated around 0.7, practically invariant with temperature indicate that transport mechanism of cations and anions does not change with temperature.

Nevertheless, to better understand the transport mechanism, the diffusion coefficients for CO_3^{2-} will be measured using ^{13}C enriched carbonate. Other eutectic mixtures of carbonates such as $\text{Li}_2\text{CO}_3\text{-K}_2\text{CO}_3$, $\text{Li}_2\text{CO}_3\text{-Na}_2\text{CO}_3\text{-K}_2\text{CO}_3$ and $\text{Na}_2\text{CO}_3\text{-K}_2\text{CO}_3$ will be studied at high temperature to provide some additional data in order to constraint the different model given by molecular dynamic simulations.

Acknowledgements:

This work was funded by the French National Research Agency (ANR-11-EAPX-0036 project MCEC).

References:

- [1] S. M. Benson and F. M. Orr, *Carbon dioxide capture and storage*, vol. 33, no. 4. 2008.
- [2] Fuel Cell Today, D. Carter, and J. Wing, "The Fuel Cell Industry Review 2013," 2013.
- [3] Y. Kono *et al.*, "Ultralow viscosity of carbonate melts at high pressures," *Nat. Commun.*, vol. 5, pp. 1–8, 2014.
- [4] A. P. Jones, M. Genge, and L. Carmody, "Carbonate melts and carbonatites," *Rev. Mineral. Geochemistry*, vol. 75, no. Wyllie 1995, pp. 289–322, 2013.
- [5] L. Bonafous, B. Ollivier, Y. Auger, H. Chaudret, C. Bessada, D. Massiot, I. Farnan, J.P. Coutures "High temperature NMR observation of mobile phases up to 1500 ° C" *J. Chim. Phys.*, pp. 1867–1870, 1995.
- [6] F. Gaillard, M. Malki, G. Iacono-Marziano, M. Pichavant, and B. Scaillet, "Carbonatite melts and electrical conductivity in the asthenosphere," *Science (80-.)*, vol. 322, no. 5906, pp. 1363–1365, 2008.
- [7] A. L. Rollet, V. Sarou-Kanian, and C. Bessada, "Measuring self-diffusion coefficients up to 1500 K: A powerful tool to investigate the dynamics and the local structure of inorganic melts," *Inorg. Chem.*, vol. 48, no. 23, pp. 10972–10975, 2009.
- [8] P. L. Spedding and R. Mills, "Trace-Ion Diffusion in Molten Alkali Carbonates," *J. Electrochem. Soc.*, vol. 112, no. 6, pp. 594–599, 1965.
- [9] V. Lacassagne, C. Bessada, B. Ollivier, D. Massiot, P. Florian, and J. P. Coutures, "Study of the solide/liquid transition of the cryolite by nuclear magnetic resonance of ²⁷Al, ²³Na et ¹⁹F" *Comptes Rendus l'Académie des Sci. - Ser. IIB*, vol. 325, no. 2, pp. 91–98, 1997.
- [10] K. Machado *et al.*, "Study of NaF-AlF₃ Melts by Coupling Molecular Dynamics, Density Functional Theory, and NMR Measurements," *J. Phys. Chem. C*, vol. 121, no. 19, pp. 10289–10297, 2017.
- [11] N. F. Ostrovskaya, T. S. Bartnitskaya, V. I. Lyashenko, V. B. Zelyavskii and A. V. Kurdyumov, "Crystallization of boron nitride from solution in a lithium borate melt", *Powder metallurgy and metal ceramics*, vol. 35, no. 392, pp. 636–639, 1997.

- [12] S. Gál, K. Tomor, E. Pungor, G. Soóki-Tóth, and P. Horváth, "Reactions of binary and ternary alkali metal carbonate mixtures with aluminium oxide," *J. Therm. Anal.*, vol. 9, no. 2, pp. 241–250, 1976.
- [13] A. L. Rollet, V. Sarou-Kanian, and C. Bessada, "Self-diffusion coefficient measurements at high temperature by PFG NMR," *Comptes Rendus Chim.*, vol. 13, no. 4, pp. 399–404, 2010.
- [14] A. Jerschow and N. Müller, "Convection Compensation in Gradient Enhanced Nuclear Magnetic Resonance Spectroscopy," *J. Magn. Reson.*, vol. 132, no. 1, pp. 13–18, 1998.
- [15] P. L. Spedding and R. Mills, "Tracer Diffusion Measurements in Mixtures of Molten Alkali Carbonates," *J. Electrochem. Soc.*, vol. 113, no. 6, pp. 599–603, 1966.
- [16] C. Simonnet, J. Phalippou, M. Malki, and A. Grandjean, "Electrical conductivity measurements of oxides from molten state to glassy state," *Rev. Sci. Instrum.*, vol. 74, no. 5, pp. 2805–2810, 2003.
- [17] Y. Miyazaki, M. Yanagida, K. Tanimoto, T. Kodama and S. Tanase, "An Apparatus for Electrical Conductance Measurements with Molten Carbonates," *J. Electrochem. Soc.*, vol. 133, no. 7, pp. 1402-1404, 1986.
- [18] V. Lair, V. Albin, A. Ringuède, M. Cassir, "Theoretical predictions vs. experimental measurements of the electrical conductivity of molten $\text{Li}_2\text{CO}_3\text{-K}_2\text{CO}_3$ modified by additives," *J. Hydrogen Energy*, vol. 7, pp. 3–10, 2011.
- [19] E. Desmaele, N. Sator, R. Vuilleumier, and B. Guillot, "Atomistic simulations of molten carbonates: Thermodynamic and transport properties of the $\text{Li}_2\text{CO}_3 - \text{Na}_2\text{CO}_3 - \text{K}_2\text{CO}_3$ system," *J. Chem. Phys.*, vol. 150, no. 9, 2019.
- [20] W. Hai-jun, "Ion Potential Principle Summary," *London Journal of Research in science: Natural and Formal*, vol. 19, no. 2, 2019.
- [21] P. Abelard and J. F. Baumard, "Dielectric relaxation in alkali silicate glasses: A new interpretation," *Solid State Ionics*, vol. 14, no. 1, pp. 61–65, 1984.
- [22] T. Yoshino, B. Gruber, and C. Reinier, "Effects of pressure and water on electrical conductivity of carbonate melt with implications for conductivity anomaly in continental mantle lithosphere," *Phys. Earth Planet. Inter.*, vol. 281, pp. 8–16, 2018.

- [23] T. Kojima, Y. Miyazaki, K. Nomura, and K. Tanimoto, "Physical Properties of Molten $\text{Li}_2\text{CO}_3\text{-Na}_2\text{CO}_3$ (52:48 mol%) and $\text{Li}_2\text{CO}_3\text{-K}_2\text{CO}_3$ (62:38 mol%) Containing Additives," *J. Electrochem. Soc.*, vol. 160, no. 10, pp. H733–H741, 2013.

Table captions:

Table 1. Fit parameters of equation (1) and comparison with Kojima et al. values [23].

Table 2. Ideal electrical conductivity (σ^{NE}) calculated at different temperature from self-diffusion coefficients Na^+ , Li^+ measured by PFG NMR ; $\text{D}_{(\text{CO}_3^{2-})}$ measured by Spedding et al. [15], σ (S/m) measured by 4-electrode system in this work, and Haven ratio [19] ($H = \sigma^{NE} / \sigma$).

	This work	Kojima et al. [23]
<i>Ea</i> (eV)	0.20 ± 0.01	0.20
ln(σ_0) ($\Omega^{-1} \cdot \text{cm}^{-1} \cdot \text{K}$)	3.28 ± 0.05	3.21

Table 1

T (K)	$D_{\text{Co}_3^{2-}}$ (m^2/s) [15]	σ^{NE} (S/m)	σ (S/m)	H
861	$7 \cdot 10^{-10}$	212	177.3	0.8
952	$1.73 \cdot 10^{-9}$	329	230.3	0.7
1008	$2.24 \cdot 10^{-9}$	385	267.9	0.7

Table 2

Figure captions:

Figure 1. System of two crucibles for NMR measurements; alumina crucible (creamy colour), magnesium oxide crucible with plug (grey colour).

Figure 2. a) ^{23}Na ($I=3/2$) and b) ^7Li ($I=3/2$) NMR spectra at different temperatures for the $\text{Li}_2\text{CO}_3\text{-Na}_2\text{CO}_3$ (52:48 %mol) eutectic point.

Figure 3. Evolution of ^{23}Na (black filled squares) and ^7Li (black empty squares) chemical shifts with temperature for the $\text{Li}_2\text{CO}_3\text{-Na}_2\text{CO}_3$ (52:48 %mol) eutectic point.

Figure 4. ^{23}Na and ^7Li diffusion coefficient in $\text{Li}_2\text{CO}_3\text{-Na}_2\text{CO}_3$ (52:48 %mol) eutectic mixture.

Figure 5. Arrhenius plots from ^7Li (green squares) and ^{23}Na (black squares) NMR diffusion coefficients for $\text{Li}_2\text{CO}_3\text{-Na}_2\text{CO}_3$ (52:48 %mol) eutectic mixture.

Figure 6. Cole-Cole representation of the complex impedance $\text{Li}_2\text{CO}_3\text{-Na}_2\text{CO}_3$ (52:48 %mol) eutectic point at different temperatures.

Figure 7. Comparison of the electrical conductivity measured with the 4-electrode system (squares and plain line) and electrical conductivity obtained by calculations from Kojima et al. [23] (dashed line).

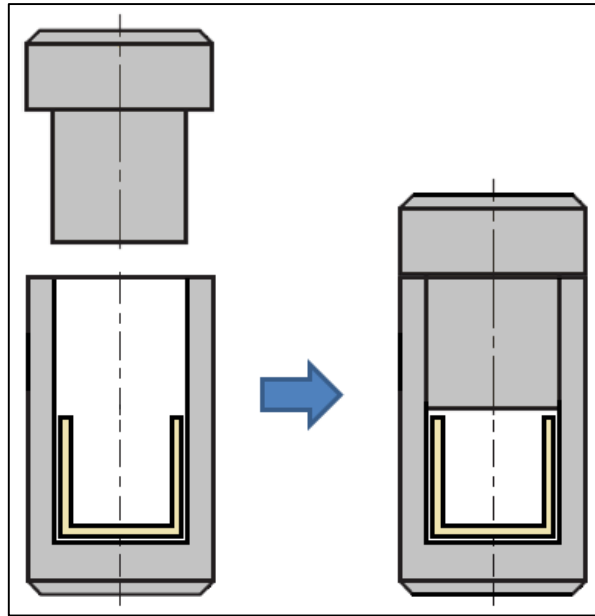


Fig.1

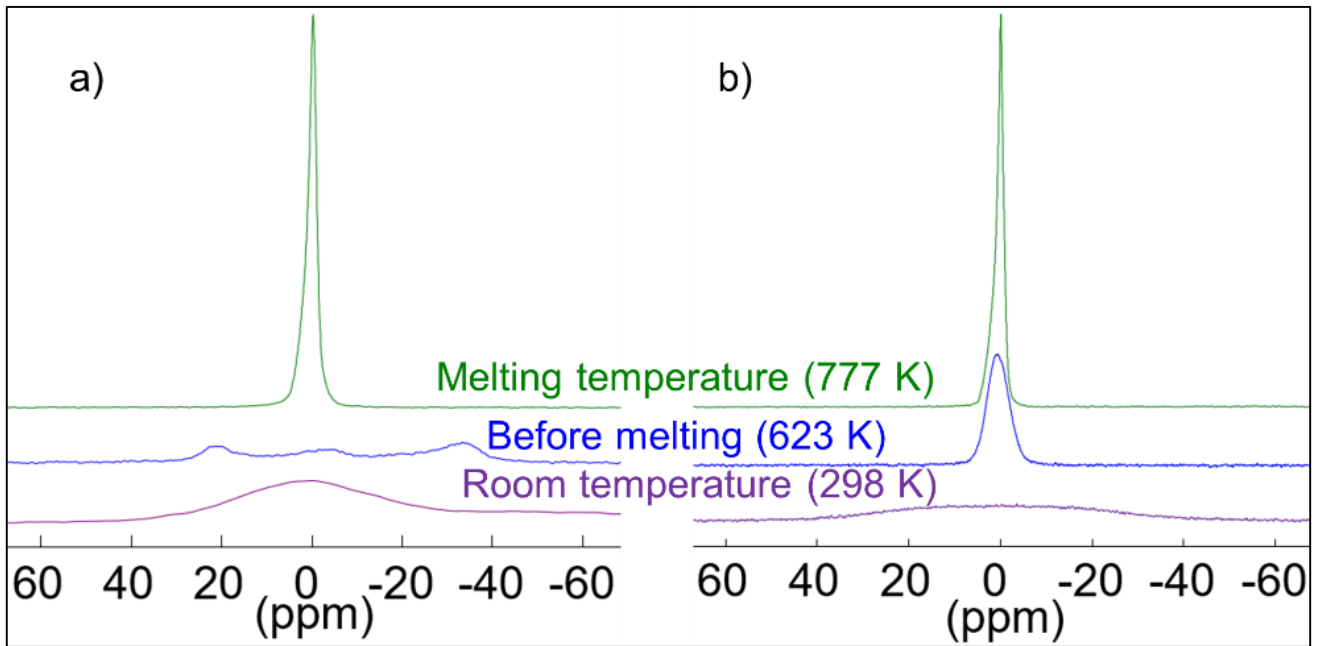


Fig.2

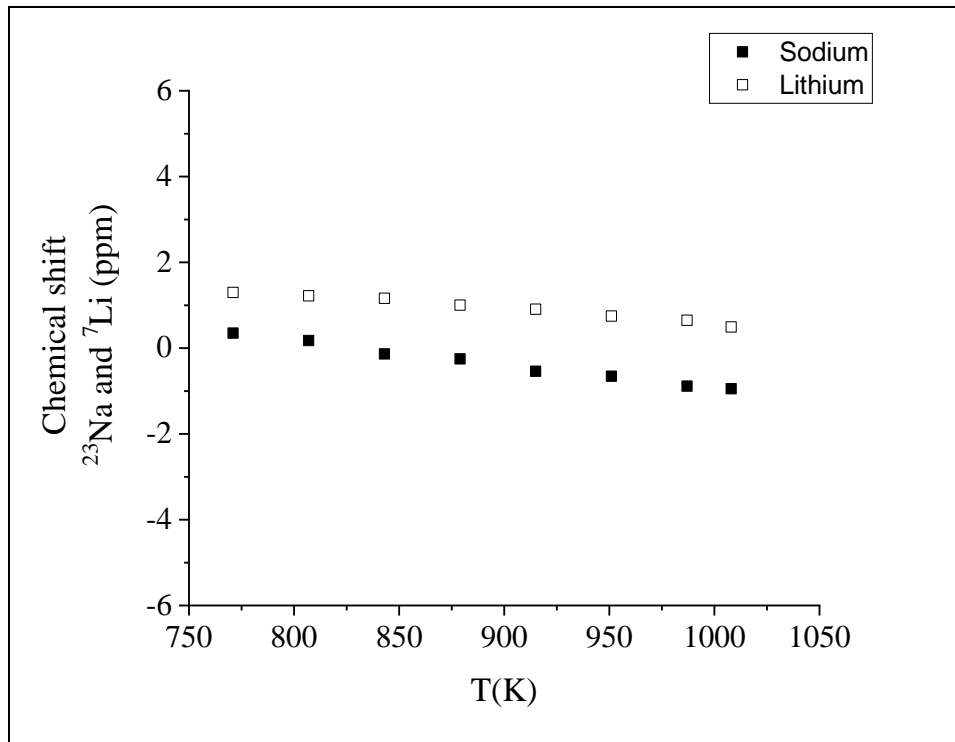


Fig.3

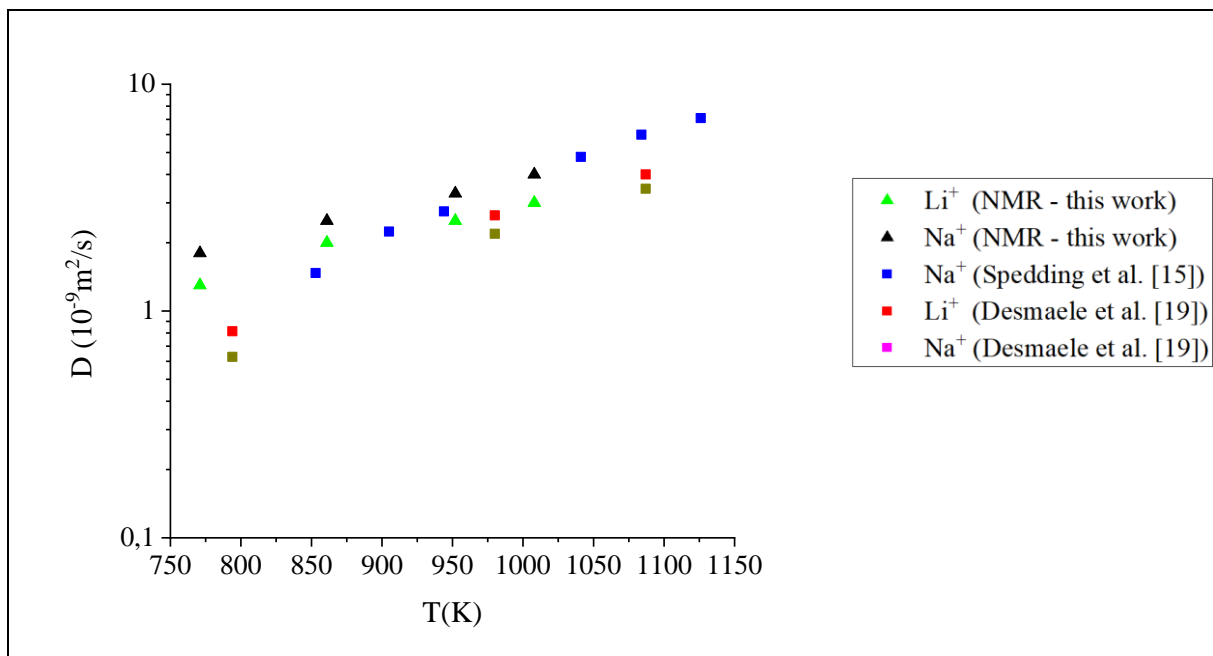


Fig.4

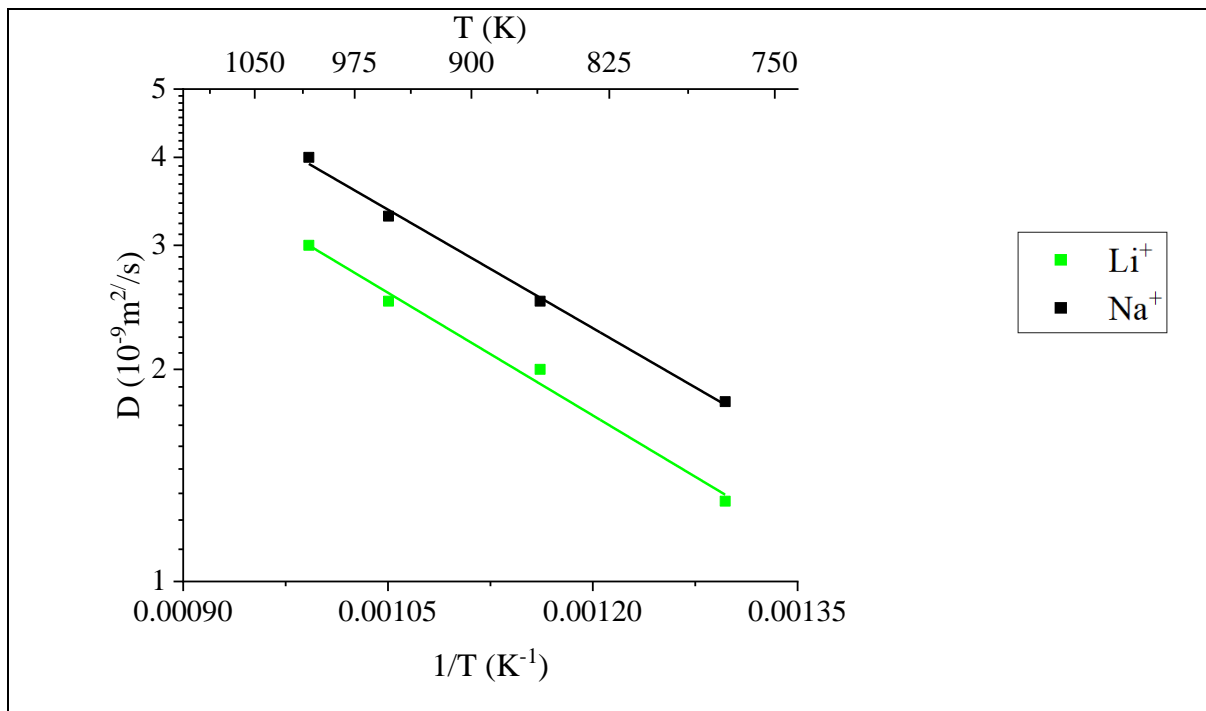


Fig.5

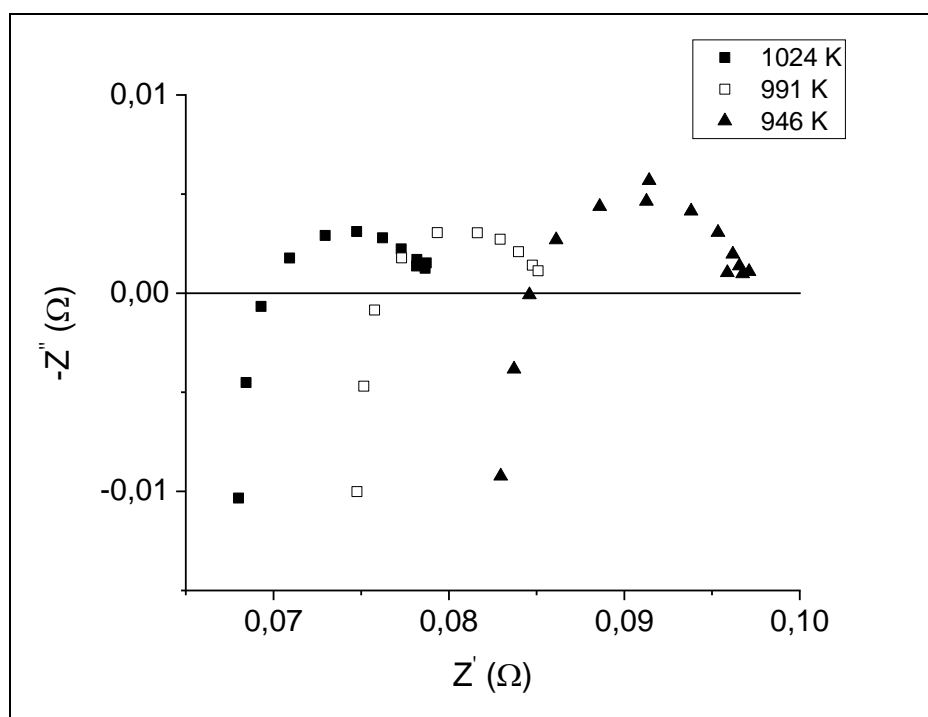


Fig.6

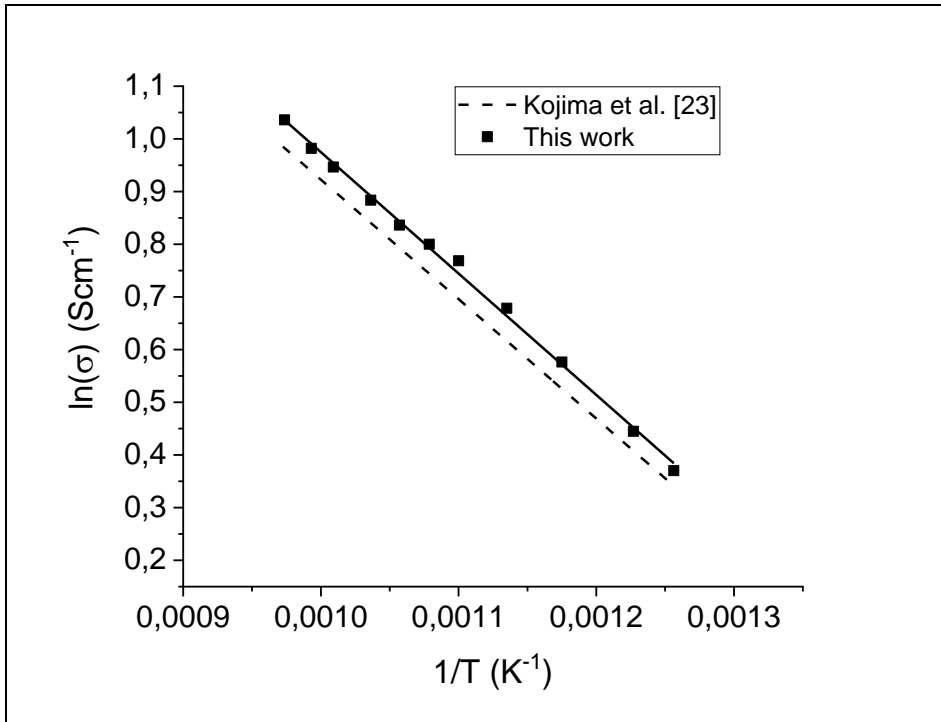


Fig.7